MEDDOCS Open Access Publisher

Nanoscience and Nanotechnology: Open Access

Open Access | Review Article

The Influence of Silver and Copper Nanoparticles on the Optical Properties of Photochromic Molecules

Frederik Ørsted Kjeldal[#]; Andreas Erbs Hillers-Bendtsen[#]; Kurt V Mikkelsen*

Department of Chemistry, University of Copenhagen, Universitetsparken 5, 2100 Copenhagen O, Denmark.

[#]These authors contributed equally to this work.

Corresponding Author(s): Kurt V Mikkelsen

Department of Chemistry, University of Copenhagen, Universitetsparken 5, 2100 Copenhagen O, Denmark.
Email: kmi@chem.ku.dk

Received: Sep 10, 2023

Accepted: Dec 13, 2023

Published Online: Dec 20, 2023

Journal: Nanoscience and Nanotechnology: Open Access

Publisher: MedDocs Publishers LLC

Online edition: http://meddocsonline.org/

Abstract

The focus of this paper is on the optical properties, in particular the vertical excitations and two-photon excitations, of the 3-amino-substituted dihydroazulene/vinylheptafulvene system and how they change when the system is physisorbed onto a nanoparticle. Di- hydroazulene, s-cis-vinylheptafulvene and s-trans-vinylheptafulvene were orientated in different ways and at different distances to silver and copper nanoparticles to see how this would affect the optical properties. A combined quantum mechanical/molecular mechanical method was used for these calculations with the molecules being treated quantum mechanically, specifically using linear and quadratic response theory within time-dependent density functional theory, while the nanoparticles were treated classically, each being assigned a static polarizability for each atom of the nanoparticles. The calculations were carried out using the polarizable embedding scheme, along with the long-range corrected functional, CAM-B3LYP and the augmented correlation con- sistent basis set, aug-cc-pVDZ. It was found that the nanoparticles affected the molecules differently, with the copper nanoparticle generally influencing the optical properties the most. It was found that the relative orientation of the different molecules had a very large impact on the effect of the nanoparticles. It was also found that in general, the dihydroazulene was affected the least by both nanoparticles and s-trans-vinylheptafulvene was affected the most.

Introduction

The 3-amino-substituted dihyrdoazulene(DHA)/vinylheptafulvene(VHF) is a photochromic system, with the parent DHA/VHF system being synthesized for the first time by Daub in 1984 [1]. The parent system is the DHA/VHF system seen in Figure 1, but with the amino group replaced by a hydrogen. This photochromic system, along with other photochromic systems have been studied for their use in many different applications including data storage, chemical solar cells, molecular switches, and molecular electronics [2-25]. It is important to study the use of the photochromic systems for the above mentioned applications as they may allow more compact technologies, such as molecular electronics which then allows for faster calculation capabilities or the application of chemical solar cells which could help alleviate the increasing global energy demand [26]. The 3-amino-substituted DHA/VHF system was found to have the highest solar energy storage capability in a previous paper [27,28] and this is the reason it was chosen for this study. Under an electronic

Cite this article: Kjeldal FØ, Hillers-Bendtsen AE, Mikkelsen KV. The Influence of Silver and Copper Nanoparticles on the Optical Properties of Photochromic Molecules. Nanosci Nanotechnol Open Access. 2023; 2(2): 1018.

excitation, the DHA molecule can ring-open and convert to the metastable molecule, s-cis-VHF. The s-trans-VHF molecule is the thermally more stable molecule, which the s-cis-VHF can thermally interconvert to. The reaction from s-trans-VHF to s-cis-VHF and the further reaction back to DHA are both thermally induced.

This reaction scheme can be seen in Figure 1. The overall reaction from s-trans-VHF to DHA releases energy which allows for the chemical storage of solar energy in this system.

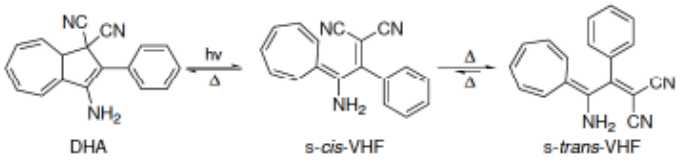

Figure 1: The structure and reaction scheme of the studied 3-amino-substituted DHA/VHF photo- and thermoswitch.

Releases energy which allows for the chemical storage of solar energy in this system.

Introducing a nanoparticle to the DHA/VHF system could allow for a perturbation of the molecular properties of the system and thus the possibility of tuning the properties for a desired application [29-33]. Nanoparticles have previously been shown to have very useful applications in e.g. controlling drug release [30,32], doing active switching of photochromic systems via excitation of the nanoparticle [31], and also either catalyzing or inhibiting photo isomerization for some systems chemisorbed onto nanoparticles [29,33]. Previous papers have studied the influence of a gold nanoparticle on this specific system and found some interesting results where the molecular properties can be changed by the nanoparticle [34,35]. This paper considers silver and copper nanoparticles since they represent cheaper alternatives to gold nanoparticles if the molecular properties can be altered similarly.

The optical properties are, of course, very relevant to the application of DHA/VHF as a chemical solar cell and will therefore be the focus of this paper. We will, in particular, look at the vertical excitation energies and associated oscillator strengths, along with the two-photon excitations when DHA, s-*cis*-VHF and s-*trans*-VHF are influenced by a silver or copper nanoparticle. The main questions we are seeking to answer are which nanoparticle has the greatest effect on the optical properties? How important is the relative orientation of the molecule with respect to the nanoparticle? If important, which orientation gives rise to the greatest effect of the nanoparticles on the molecular systems? How important is the molecule-nanoparticle distance? Which molecule is the most affected by the influence from that nanoparticle?

Computational approach

The calculations of the optical properties of the DHA/VHF system were done using the combined quantum mechanical (QM)/molecular mechanics (MM) method [36-40] using the electronic structure program Dalton 16 [41]. In this method, we split the system into two subsystems where one is described by classical mechanics, for the non chemically interesting part, the nanoparticle. And a subsystem which is described by quantum mechanics, the chemically interesting part of the system. The two subsystems interact through the polarizable embedding (PE) scheme, which allow the subsystems to polarize one another.

The QM part, DHA, s-*cis*-VHF and s-*trans*-VHF, were optimized using vacuum DFT in the electronic structure program Gaussian09 [42] using the long-range corrected CAM-B3LYP functional [43] and the augmented correlation consistent basis set aug-cc-pVDZ [44]. This procedure has been documented previously to be sufficiently accurate for describing physisorbed molecules interacting with nanoparticles [45].

The nanoparticles were constructed as hemispheres consisting of 70 atoms and their geometries were kept constant. This is to allow comparison to previous papers with gold nanoparticles [34,35] and as a change in size and geometry of the nanoparticle have been shown to have only a small effect on the studied molecular properties [34,35,45]. The coordination surface was a fcc (111) surface as this has been shown to be the most likely site for the coordination of the molecules [46,47]. Each atom was prescribed a static polarizability of 49.9843 au [48] for the silver atoms and 33.742 au [49-51] for the copper atoms. This also means that the optical properties of the nanoparticles were not included. The copper nanoparticle had a smaller bond-length within the nanoparticle as compared to the silver nanoparticle, being 2.556 Å and 2.889 Å, respectively.

The molecules were then physisorbed onto the nanoparticle, in four different orientations, the 7-membered, phenyl, cyano, and amino orientation, which can be seen in Figure 2, at three different distances for each orientation. The closest distance was chosen to be the sum of the van der Waals radius of the atom closest to the nanoparticle and the van der Waals radius of the nanoparticle atom. For the orientations where a hydrogen was closest to the nanoparticle, the 7-membered, phenyl and amino orientations, the distances were 2.92 **Å** and 2.60 Å for the silver nanoparticle and the copper nanoparticle, respectively. For the orientation where a nitrogen was closest, the cyano orientation, the distances were 3.27 Å and 2.95 Å for the silver nanoparticle and the copper nanoparticle, respectively. Each distance was then increased twice, in steps of 1 Å. However, for the s-*cis*-VHF in the amino and cyano orientations and for the s-*trans*-VHF in the amino orientation had convergence issues in the PE calculations for the closest distance, when physisorbed onto the copper nanoparticle. The shortest distances were then increased in steps of 0.05 Å until convergence was achieved. This was achieved at distances of 3.10 Å and 3.15 Å for the s-*cis*-VHF in the amino and cyano orientations, respectively. The amino orientation for the s-*trans*-VHF converged at a shortest distance of 2.80 Å. The two other distances were still increased in steps of 1 Å from the sum of the van der Waals radii, even if the shortest distance did not converge.

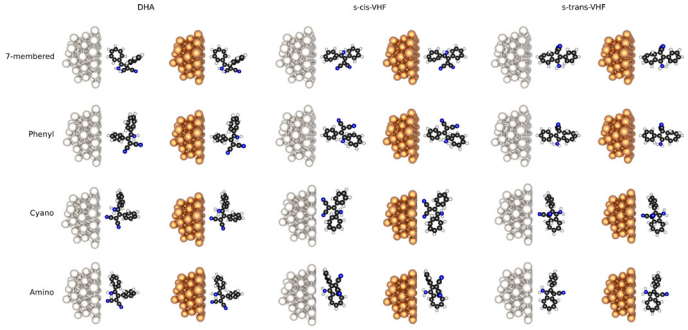

Figure 2: The different orientations for each molecule physisorbed onto the silver nanoparticle and the copper nanoparticle at a distance of 3.00 Å.

After the PE calculations converged we move on to calculate the optical properties, which were chosen as the first 15 vertical excitation energies and corresponding oscillator strengths, and for the first five two-photon excitations, the linear and circular two-photon absorption cross-section. This was done for all the molecules in each orientation, at the three distances to both nanoparticles. The method used was linear and quadratic response within TD- DFT, again using the long-range corrected functional, CAM-B3LYP [43] with the augmented correlation consistent basis set, aug-cc-pVDZ [44]. The poles of the linear response function provide the vertical excitation energies and the residues of the linear response function give the transition dipole moments needed to calculate the oscillator strengths. The vertical excitation energies and corresponding oscillator strengths were then used to simulate a UV- Vis spectrum by fitting to Gaussian functions. The matrix elements of the two-photon transition dipoles are calculated from the residue of the quadratic response function and used for calculating the two-photon absorption cross section.

$$\delta^{TPA} = \frac{1}{30}\sum_{\alpha,\beta}\left(S_{\alpha,\alpha}S_{\beta,\beta}F + S_{\alpha,\beta}S_{\alpha,\beta}G + S_{\alpha,\beta}S_{\beta,\alpha}H\right) \quad (1)$$

where $S_{\alpha,\beta}$ is the matrix elements in various Cartesian components, α and β, and F, S, and G being different constants related to either linear or circular polarized light.

Results

One-photon: In this section we present the investigations of the effects of the nanoparticles onto the physisorbed molecules. We start out by presenting the results for DHA followed by the ones for VHF in the cis and trans conformations. For each molecule we present results for the four different orientations and distances.

DHA: The UV-Vis spectra for the DHA molecules in each orientation and on both the silver nanoparticle and the copper nanoparticle are shown in Figures 3-10.

Table 1: Excitation wavelength change for each of the first [15] excitations when moving from the closest to the furthest molecule-nanoparticle distance for DHA in the 7-membered orientation for both the silver nanoparticle and the copper nanoparticle.

Ex. no.	Ag[nm]	Cu[nm]
1	1.158	0.633
2	0.055	0.202
3	0.199	0.111
4	0.219	0.172
5	0.024	-0.712
6	0.082	0.213
7	-0.033	0.115
8	-0.574	-0.728
9	0.392	0.478
10	0.502	0.411
11	0.515	0.257
12	-0.281	-0.062
13	0.154	0.477
14	1.384	0.810
15	0.256	0.010

Starting with Figures 3 and 4, which is the 7-membered orientation, we do not observe any redshift when moving towards the nanoparticle, but there is a slight increase in absorption for both the silver nanoparticle and the copper nanoparticle. In Table 1, we see the difference in excitation wavelength between the closest and furthest molecule-nanoparticle distance. We see primarily small increases in the wavelengths for both the silver nanoparticle and copper nanoparticle with increasing distance between the molecule and the nanoparticle.

Table 2: Excitation wavelength change for each of the first 15 excitations when moving from the closest to the furthest molecule-nanoparticle distance for DHA in the phenyl orientation for both the silver nanoparticle and the copper nanoparticle.

Ex. no.	Ag[nm]	Cu[nm]
1	1.300	1.306
2	0.251	0.247
3	0.193	0.266
4	-0.134	0.079
5	0.172	-0.524
6	0.067	0.141
7	0.164	0.471
8	0.129	-0.157
9	0.249	0.453
10	0.315	0.504
11	0.153	0.067
12	0.264	0.323
13	0.166	0.382
14	0.268	0.342
15	0.134	0.021

We see similar tendencies in the UV-Vis spectra for phenyl orientations, Figures 5 and 6. That is small increases in the wavelength as the separation distance is increased. There is no significant redshift, but we see a slightly larger increase in absorption for the silver nanoparticle as compared to the copper nanoparticle. The table of differences in wavelength, Table 2, shows a similar increase in wavelength as for the 7-membered orientation.

For the UV-Vis spectra for the cyano orientations, Figures 7 and 8, we see a redshift of 4 nm with the copper nanoparticle. The copper nanoparticle leads to the largest increase in absorption intensities whereas the silver nanoparticle gives a small increase in the intensities. In Table 3 we see increases in the absorption wavelengths as well, and they are generally

larger than for the previous orientations, especially for the copper nanoparticle. The UV-Vis spectra of the amino orientations, Figures 9 and 10, exhibit the largest redshift for the DHA molecule. This is again for the molecule with the copper nanoparticle which has a redshift of 8 nm in this case. The silver nanoparticle also provided a redshift in this case of 6 nm, but does not show a real increase in the intensity of absorption. However, the absorption increase is very large for the copper nanoparticle. Table 4 shows only increases in wavelengths for this orientation, and we note large increases of up to around 11 nm.

Table 3: Excitation wavelength change for each of the first 15 excitations when moving from the closest to the furthest molecule-nanoparticle distance for DHA in the cyano orientation for both the silver nanoparticle and the copper nanoparticle.

Ex. no.	Ag[nm]	Cu[nm]
1	1.432	3.899
2	0.047	0.233
3	0.210	-0.018
4	0.244	0.172
5	-1.479	-1.367
6	0.525	0.618
7	1.331	1.236
8	-0.860	-1.196
9	2.786	1.935
10	0.942	1.677
11	0.221	-0.180
12	0.120	0.365
13	1.518	1.637
14	-0.028	-0.488
15	-1.052	-0.921

***s-cis*-VHF**

We now move onto the *s-cis*-VHF, for all orientations and on both nanoparticles and the UV-Vis spectra can be seen in Figures 12-18.

The 7-membered orientation, Figures 11 and 12, show a redshift in the first absorption band of around 5 nm for the silver nanoparticle and 4 nm for the copper nanoparticle. We also see a slight increase in absorption for both nanoparticles as well. Looking at Table 5, we see almost only positive wavelength changes again, with the silver nanoparticle having the largest increases of the wavelengths.

Table 4: Excitation wavelength change for each of the first 15 excitations when moving from the closest to the furthest molecule-nanoparticle distance for DHA in the amino orientation for both the silver nanoparticle and the copper nanopar ticle.

Ex. no.	Ag[nm]	Cu[nm]
1	5.500	8.153
2	6.367	10.585
3	7.932	4.772
4	5.449	6.220
5	10.965	9.432
6	2.189	6.390
7	3.360	9.497
8	5.714	7.694
9	3.639	5.406
10	2.157	1.904
11	2.607	0.957
12	2.088	2.229
13	3.053	3.234
14	5.054	5.027
15	2.640	4.768

Table 5: Excitation wavelength change for each of the rst 15 excitations when moving from the closest to the furthest molecule-nanoparticle distance for *s-cis*-VHF in the 7-membered orientation for both the silver nanoparticle and the copper nanoparticle.

Ex. no.	Ag[nm]	Cu[nm]
1	5.243	3.888
2	-1.247	0.620
3	0.609	0.393
4	1.220	0.533
5	2.438	0.171
6	-0.067	0.283
7	1.554	0.373
8	1.306	0.393
9	2.803	1.293
10	0.892	0.857
11	3.972	-0.198
12	2.511	0.634
13	0.929	0.143
14	1.084	0.586
15	0.027	0.154

Table 6: Excitation wavelength change for each of the rst 15 excitations when moving from the closest to the furthest molecule-nanoparticle distance for *s-cis*-VHF in the phenyl orientation for both the silver nanoparticle and the copper nanoparticle.

Ex. no.	Ag[nm]	Cu[nm]
1	5.243	3.888
2	-1.247	0.620
3	0.609	0.393
4	1.220	0.533
5	2.438	0.171
6	-0.067	0.283
7	1.554	0.373
8	1.306	0.393
9	2.803	1.293
10	0.892	0.857
11	3.972	-0.198
12	2.511	0.634
13	0.929	0.143
14	1.084	0.586
15	0.027	0.154

The UV-V is spectra for the phenyl orientation, Figures 13 and 14, show no redshift and no real change in the absorption intensities for both nanoparticles. This is also seen in Table 6, where we have both increases and decreases in wavelength, all of which are minuscule in magnitude.

At the cyano orientation, Figures 15 and 16, we see redshifts for both nanoparticles. For the silver nanoparticle we see a redshift of 21 nm for the first absorption band. There is also an increase in absorption for both of the larger absorption bands. For the copper nanoparticle, the first absorption band has a large increase in absorption, while the tall absorption band has

a slight increase. The first absorption band is also redshifted 47 nm for the copper nanoparticle. Table 7 shows the large increase in the wavelength excitation for this orientation. The copper nanoparticle especially has large increases for almost all excitations.

Table 7: Excitation wavelength change for each of the rst 15 excitations when moving from the closest to the furthest molecule-nanoparticle distance for *s-cis*-VHF in the cyano orientation for both the silver nanoparticle and the copper nanoparticle.

Ex. no.	Ag[nm]	Cu[nm]
1	20.355	47.653
2	-4.614	-8.669
3	2.862	5.794
4	1.779	3.186
5	0.926	3.086
6	1.383	1.398
7	3.570	9.874
8	3.265	9.376
9	0.723	6.856
10	4.201	9.721
11	7.876	8.750
12	-0.216	6.861
13	2.702	5.370
14	1.267	3.266
15	0.628	1.522

For the amino orientation, we observe from Fig. 17, 18 and Table 8, some increases when the molecule is near the nanoparticle. The UV-Vis spectra show a redshift of 10 nm for the silver nanoparticle and 8 nm for the copper nanoparticle, for the first absorption band. We, however, see a decrease in absorption for the tall peak for the silver nanoparticle and a smaller decrease for the same peak for the copper nanoparticle UV-Vis spectrum. The first absorption band, however, shows increases in absorption for both nanoparticles. The difference in excitation wavelengths is positive for all excitations for both nanoparticles and we generally observe signifcant increases.

***s-trans*-VHF**

The last one-photon results are for the s-trans-VHF molecule, and the UV-Vis spectra can be seen in Figures 19-26. Starting with the 7-membered orientation, Figures 19 and 20, where there is a redshift of 8 nm and 11 nm for the silver nanoparticle and the copper nanoparticle, respectively, for the first absorption band. We see a slight increase in absorption, which is similar for the two nanoparticles. Table 9 shows both increases and decreases in excitation wavelength almost all being of small magnitude.

The phenyl orientation on the silver nanoparticle, Figure 21, shows no redshift and no increase in absorption. However, on the copper nanoparticle, Figure 22, we see a redshift of the first absorption band of 4 nm along with a slight increase in absorption for both peaks. The table of excitation wavelengths for the phenyl orientation, Table 10, shows both increases and decreases in excitation wavelength for both nanoparticles. The magnitudes are also small with the largest increase being around 2 nm for both nanoparticles as well. For the cyano orientations of

Table 8: Excitation wavelength change for each of the first 15 excitations when moving from the closest to the furthest molecule-nanoparticle distance for *s-cis*- VHF in the amino orientation for both the silver nanoparticle and the copper nanoparticle.

Ex. no.	Ag[nm]	Cu[nm]
1	9.833	8.097
2	5.362	0.813
3	3.887	9.189
4	9.741	11.881
5	8.541	15.368
6	0.579	5.994
7	4.100	4.860
8	2.400	2.279
9	7.640	4.719
10	0.949	3.531
11	3.600	4.531
12	1.311	1.633
13	2.020	2.832
14	2.166	2.717
15	1.226	1.053

Table 9: Excitation wavelength change for each of the first 15 excitations when moving from the closest to the furthest molecule-nanoparticle distance for s- trans-VHF in the 7-membered orientation for both the silver nanoparticle and the copper nanoparticle.

Ex. no.	Ag[nm]	Cu[nm]
1	2.910	5.045
2	-0.986	-0.127
3	-0.361	-0.194
4	0.964	2.072
5	-0.381	-0.364
6	1.006	0.929
7	0.656	0.867
8	0.120	0.311
9	0.994	0.904
10	-1.029	-1.223
11	0.427	0.606
12	-0.213	0.047
13	0.750	0.754
14	0.003	0.502
15	0.130	0.206

s-cis-VHF, Fig. 23 and 24, we see redshifts as well. We observe a redshift of 13 nm for the silver nanoparticle and 25 nm for the copper nanoparticle for the first absorption band. We observe a larger increase in the absorption intensities for the copper nanoparticle of the rst absorption band but a larger increase for the silver nanoparticle for the tall peak. The changes to excitation wavelengths, Table 11, show both decreases and increases, but mostly increases for both nanoparticles. The magnitudes of most of these changes are quite small except for the firrst excitation.

Table 10: Excitation wavelength change for each of the first 15 excitations when moving from the closest to the furthest molecule-nanoparticle distance for *s- trans*-VHF in the phenyl orientation for both the silver nanoparticle and the copper nanoparticle.

Ex. no.	Ag[nm]	Cu[nm]
1	0.314	2.318
2	-0.303	-0.390
3	2.060	1.960
4	-0.713	-0.281
5	1.007	1.187
6	0.264	-0.071
7	-0.969	-0.633
8	-0.375	-0.009
9	-0.091	-0.605
10	0.214	-0.199
11	0.767	0.222
12	0.543	0.368
13	0.769	-0.005
14	-0.306	-0.724
15	0.233	0.189

Table 11: Excitation wavelength change for each of the first 15 excitations when moving from the closest to the furthest molecule-nanoparticle distance for *s-trans*-VHF in the cyano orientation for both the silver nanoparticle and the copper nanoparticle.

Ex. no.	Ag[nm]	Cu[nm]
1	6.548	16.250
2	-2.696	-1.873
3	1.928	1.523
4	0.008	1.631
5	2.027	1.281
6	-0.738	-0.986
7	-0.953	0.737
8	0.306	2.343
9	-0.048	-1.059
10	-1.538	-1.215
11	1.453	3.027
12	0.169	-0.835
13	-0.438	0.283
14	-0.577	-0.174
15	0.490	0.812

The last UV-Vis spectra are for the amino orientation, Figures 25 and 26, which are very different when comparing the silver nanoparticle and the copper nanoparticle. The silver nanoparticle has a redshift of 19 nm while the redshift is 74 nm for the copper nanoparticle for the first absorption band. The largest increase in absorption intensity is also observed here for the copper nanoparticle. The absorption intensity for the silver nanoparticle also increases and this is similar to the other orientations. The table of excitation wavelengths also show large increases, the largest being 84 nm for the silver nanoparticle and 67 nm for the copper nanoparticle. All the excitation wavelengths also increase except the second excitation for the copper nanoparticle. The magnitudes of the changes are in general quite large.

In summary, we observe the greatest effects of the nanoparticles for the cyano and amino orientations and the largest changes were generally caused by the copper nanoparticle. Both VHF molecules are more affected by the nanoparticle compared to the DHA, with the s-trans-VHF molecule being affected the most overall. In general, the absorption of the molecule increases when close to the nanoparticle, but we have some cases where we observe a redshift with no real increase in absorption as seen in Figure 17.

Table 12: Excitation wavelength change for each of the first 15 excitations when moving from the closest to the furthest molecule-nanoparticle distance for *s- trans*-VHF in the amino orientation for both the silver nanoparticle and the copper nanoparticle.

Ex. no.	Ag[nm]	Cu[nm]
1	16.930	67.182
2	6.020	-15.023
3	83.749	5.101
4	11.002	6.847
5	19.346	21.672
6	3.165	10.955
7	6.028	20.122
8	4.054	9.644
9	9.075	13.764
10	5.500	12.264
11	3.137	10.054
12	1.946	5.823
13	1.850	4.100
14	1.567	3.837
15	0.649	1.115

Two-photon

DHA

For the two-photon process, we can see in Table 13 the two-photon absorption (TPA) crosssection for all orientations of DHA with the silver nanoparticle. We see that there is only a small change in TPA for the 7-membered orientation on the silver nanoparticle. We observe that in general the TPA decreases when increasing the molecule-nanoparticle distance by 1 Å and the TPA increases when increasing the distance 1 Å again. The first excitation is the exception for this. For the phenyl orientation we also observe a small change in TPA, when increasing the molecule-nanoparticle distance. Now looking at the cyano orientation, we see a similar tendency in TPA compared to the 7-membered and phenyl orientation. The amino orientation has the largest change in TPA compared to the previous orientations, having larger values for the first, fourth, and fifth excitation and then decreasing when increasing molecule-nanoparticle distance. The second and third excitations are smaller than the previous orientations and then increase when moving further away from the nanoparticle. Comparing this with the Table for the DHA molecule in all orientations with the copper nanoparticle, Table 14, we observe similar trends. The copper nanoparticle caused a much larger change in TPA for the cyano orientation, but the copper nanoparticle had the same trends as for the silver nanoparticle for this orientation. The same

trend is noticed for the amino orientation, but it is even more pronounced in this orientation. In general, the TPA increases when decreasing the molecule-nanoparticle distance for DHA.

***s-cis*-VHF**

For the s-cis-VHF molecule in all orientations on the silver nanoparticle, Table 15, we see the same trend as for the DHA molecule, with only small decreases in the TPA when increasing the molecule-nanoparticle distance for the 7-membered and phenyl orientations. This holds for all excitations, except the first linearly polarized light excitation for both orientations. For the other two orientations, the cyano and amino orientation, we observe a much larger difference in TPA when increasing the distance from the molecule to the nanoparticle. We observe a significant increase in TPA for the cyano orientation, when moving 1 Å away from the shortest distance in the fourth excitation. The greatest increase, for this molecule on the silver nanoparticle, is when looking at the amino orientation and when moving 2 Å away in the fifth excitation. Table 16 contains the TPA results for the s-cis-VHF molecule in all orientations with the copper nanoparticle, where we again see similar tendencies for the 7-membered and phenyl orientation on copper nanoparticle, as we did with the silver nanoparticle, that is small changes in TPA. However, there is a large change for the cyano orientation, where we observe an increase in TPA on the order of 10^3 for the fifth excitation when moving towards the nanoparticle. In general, the TPA values for the copper nanoparticle are larger than those for the silver nanoparticle.

Table 13: The two-photon cross-section, in a.u., of DHA with silver nanoparticle for all the orientations and molecule-nanoparticle distances.

Oriented : 7-membered

	Linear			Circular		
Ex. no	2.92 Å	3.92 Å	4.92 Å	2.92 Å	3.92 Å	4.92 Å
1	5.368	5.558	5.596	4.021	4.097	4.097
2	71.509	68.284	69.802	49.506	47.040	48.178
3	151.364	113.618	123.671	99.392	73.975	80.803
4	25.607	19.916	21.813	18.380	14.529	15.743
5	11.646	8.592	9.446	8.555	6.961	7.397

Orientation: Phenyl

	Linear			Circular		
Ex. no	**2.92 Å**	**3.92 Å**	**4.92 Å**	**2.92 Å**	**3.92 Å**	**4.92 Å**
1	6.923	6.259	5.937	4.932	4.344	4.533
2	66.767	66.767	67.146	45.713	46.092	46.282
3	144.535	113.618	122.533	95.029	74.164	80.234
4	18.399	18.285	18.437	13.884	13.562	13.733
5	8.630	8.023	8.232	7.018	6.753	6.847

Orientation: Cyano

	Linear			Circular		
Ex. no	**3.27 Å**	**4.27 Å**	**5.27 Å**	**3.27 Å**	**4.27 Å**	**5.27 Å**
1	6.620	6.146	5.880	4.514	4.856	4.306
2	68.664	71.319	68.284	47.609	49.696	47.230
3	121.584	136.000	114.566	79.665	89.718	74.733
4	19.347	19.537	19.158	14.264	14.605	14.112
5	8.536	9.124	8.232	7.018	7.151	6.847

Orientation: Amino

	Linear			Circular		
Ex. no	**2.92 Å**	**3.92 Å**	**4.92 Å**	**2.92 Å**	**3.92 Å**	**4.92 Å**
1	9.996	7.056	6.108	7.625	4.514	5.292
2	3.338	58.042	49.316	1.728	40.591	35.470
3	58.611	125.947	143.587	41.350	82.131	93.512
4	161.986	20.106	20.675	111.910	14.472	14.795
5	20.865	6.942	4.211	14.890	6.430	5.501

Table 14: The two-photon cross-section, in a.u., of DHA with copper nanoparticle for all the orientations and molecule-nanoparticle distances.

Orientation: 7-membered

	Linear			Circular		
Ex. no	**2.60 Å**	**3.60 Å**	**4.60 Å**	**2.60 Å**	**3.60 Å**	**4.60 Å**
1	5.690	5.596	5.596	4.154	4.078	4.097
2	68.664	66.008	66.767	47.230	45.333	45.902
3	140.931	113.238	121.584	91.805	73.785	79.096
4	25.417	19.727	21.434	18.038	14.321	15.440
5	10.546	8.668	9.408	7.985	7.075	7.473

Orientation: Phenyl

	Linear			Circular		
Ex. no	**2.60 Å**	**3.60 Å**	**4.60 Å**	**2.60 Å**	**3.60 Å**	**4.60 Å**
1	6.942	6.221	5.899	5.102	4.344	4.590
2	64.111	66.008	65.819	44.575	45.713	45.713
3	141.311	112.290	120.825	92.753	73.216	78.906
4	19.916	18.418	18.873	14.814	13.619	13.998
5	7.853	7.891	7.985	6.961	6.753	6.866

Orientation: Cyano

	Linear			Circular		
Ex. no	**2.92 Å**	**3.92 Å**	**4.92 Å**	**2.92 Å**	**3.92 Å**	**4.92 Å**
1	7.625	6.335	6.013	5.520	4.647	4.401
2	107.358	83.459	75.682	73.785	57.662	52.351
3	188.730	142.638	126.326	124.429	93.132	82.321
4	30.349	25.796	22.572	22.572	18.721	16.445
5	12.671	9.674	8.839	9.218	7.701	7.227

Orientation: Amino

	Linear			Circular		
Ex. no	**2.60 Å**	**3.60 Å**	**4.60 Å**	**2.60 Å**	**3.60 Å**	**4.60 Å**
1	37.177	7.341	6.354	23.520	4.647	5.349
2	135.810	63.732	57.662	88.770	44.005	40.022
3	24.658	146.053	187.782	35.849	95.598	123.291
4	430.571	23.710	29.211	282.621	17.052	20.675
5	17.166	9.332	9.143	14.833	7.682	7.701

s-trans-VHF

For the *s-trans*-VHF molecule, Table 17 contains the results for TPA in all orientations with the silver nanoparticle and we observe only small changes for the phenyl orientation when looking at the three dierent distances. For the 7-membered orientation we see both increases and decreases of the TPA when moving away from the nanoparticle. For the cyano orientation, we see a large value of the TPA for the fifth excitation which decreases as we move further away from the nanoparticle. The first three excitations do not lead to a large changes for the different distances. The amino orientation has the greatest TPA value for the third and fifth excitation at the closest distance which decreases when increasing the distance to the nanoparticle. For the copper nanoparticle, Table 18, we still see very small changes for the phenyl orientation, but the change is larger than for the silver nanoparticle. However, for the 7-membered orientation we see a large TPA for the closest distance for the fifth excitation, which again decreases when moving away from the nanoparticle. For the cyano orientation we observe a very large TPA for the fifth excitation at the closest distance, with the TPA being on the order of 10^5. This then decreases to the order of 10^2 for the furthest distance. The biggest TPA is observed for the amino orientation where the closest distance for the third, fourth and fifth excitation, are on the orders of 10^6, 10^6 and 10^9, respectively. They all decrease when increasing the molecule-nanoparticle distance.

In summary, we observe similar trends as for the one-photon section. The cyano and amino orientations are affected the most for all three molecules, with the amino orientation being the most affected for the DHA and *s-trans*-VHF molecules and the cyano orientation being the most affected for the *s-cis*-VHF molecule. The *s-trans*-VHF molecule was, again, aected the most overall. Overall, the copper nanoparticle has the greatest infuence compared to the silver nanoparticle.

Table 15: The two-photon cross-section, in a.u., of *s-cis*-VHF with silver nanoparticle for all the orientations and molecule-nanoparticle distances.

Oriented : 7-membered

	Linear			Circular		
Ex. no	2.92 Å	3.92 Å	4.92 Å	2.92 Å	3.92 Å	4.92 Å
1	51.972	46.851	44.575	34.901	33.194	38.315
2	5.652	5.425	6.108	4.666	4.514	4.970
3	24.848	23.141	31.676	36.229	34.142	43.247
4	149.467	137.517	182.661	105.272	96.736	128.413
5	10.470	10.148	10.356	13.619	13.259	13.771

Orientation: Phenyl

	Linear			Circular		
Ex. no	**2.92 Å**	**3.92 Å**	**4.92 Å**	**2.92 Å**	**3.92 Å**	**4.92 Å**
1	45.523	44.005	43.057	33.004	32.245	34.332
2	5.539	5.406	5.785	4.628	4.514	4.837
3	22.572	22.003	24.469	33.763	33.004	35.470
4	137.517	132.206	146.053	95.219	92.184	100.150
5	10.186	9.863	10.755	13.410	13.069	13.998

Orientation: Cyano

	Linear			Circular		
Ex. no	**3.27 Å**	**4.27 Å**	**5.27 Å**	**3.27 Å**	**4.27 Å**	**5.27 Å**
1	66.008	52.351	47.799	35.660	48.178	38.884
2	5.728	7.777	6.127	4.742	6.392	5.064
3	25.038	36.418	28.262	37.177	54.248	41.729
4	156.675	294.002	189.679	111.341	220.027	136.379
5	12.727	36.418	17.792	16.142	46.092	21.623

Orientation: Amino

	Linear			Circular		
Ex. no	**2.92 Å**	**3.92 Å**	**4.92 Å**	**2.92 Å**	**3.92 Å**	**4.92 Å**
1	62.973	50.265	46.661	37.746	34.901	46.851
2	6.316	5.785	8.156	5.387	4.856	7.246
3	26.555	23.900	34.522	39.453	35.849	51.024
4	152.502	151.174	80.044	110.393	104.892	78.148
5	31.676	8.839	280.725	22.572	5.766	165.779

Table 16: The two-photon cross-section, in a.u., of *s-cis*-VHF with copper nanoparticle for all the orientations and molecule-nanoparticle distances.

Orientation: 7-membered

	Linear			Circular		
Ex. no	**2.60 Å**	**3.60 Å**	**4.60 Å**	**2.60 Å**	**3.60 Å**	**4.60 Å**
1	51.972	46.471	44.385	34.711	33.194	38.505
2	5.482	5.368	4.590	4.552	4.457	3.850
3	24.658	23.330	25.986	36.229	34.332	38.505
4	146.811	136.379	169.383	103.375	95.977	120.256
5	11.419	10.375	17.982	14.662	13.619	19.916

Orientation: Phenyl

	Linear			Circular		
Ex. no	**2.60 Å**	**3.60 Å**	**4.60 Å**	**2.60 Å**	**3.60 Å**	**4.60 Å**
1	47.040	44.954	43.626	33.573	32.625	35.280
2	5.614	5.444	5.899	4.666	4.533	4.913
3	22.951	22.192	24.848	34.332	33.383	36.418
4	139.035	132.775	150.605	96.736	92.943	103.754
5	10.565	10.129	11.210	14.017	13.448	14.871

Orientation: Cyano

	Linear			Circular		
Ex. no	**2.92 Å**	**3.92 Å**	**4.92 Å**	**2.92 Å**	**3.92 Å**	**4.92 Å**
1	112.100	68.284	55.007	78.717	40.591	49.696
2	15.326	6.525	7.948	11.476	5.311	6.373
3	68.664	29.211	38.694	82.321	41.729	52.731
4	1198.770	188.161	280.725	997.710	134.293	204.853
5	12215.315	15.402	28.641	8478.642	18.797	32.245

Orientation: Amino

	Linear			Circular		
Ex. no	**2.60 Å**	**3.60 Å**	**4.60 Å**	**2.60 Å**	**3.60 Å**	**4.60 Å**
1	80.044	62.973	52.731	54.817	46.851	39.453
2	9.674	7.454	6.373	5.235	6.070	5.292
3	139.793	32.814	26.934	185.316	48.558	40.591
4	30.349	252.273	185.696	44.575	172.987	128.033
5	428.674	67.336	13.012	212.440	39.264	17.185

Table 17: The two-photon cross-section, in a.u., of *s-trans*-VHF with silver nanoparticle for all the orientations and molecule-nanoparticle distances.

Oriented : 7-membered

	Linear			Circular		
Ex. no	2.92 Å	3.92 Å	4.92 Å	2.92 Å	3.92 Å	4.92 Å
1	40.212	33.194	29.780	28.072	23.330	21.054
2	17.754	21.244	22.382	12.803	15.136	15.971
3	50.455	39.643	35.849	60.128	48.178	44.005
4	143.587	127.654	119.687	210.543	187.213	175.643
5	165.210	123.291	100.530	154.399	114.376	95.788

Orientation: Phenyl

	Linear			Circular		
Ex. no	**2.92 Å**	**3.92 Å**	**4.92 Å**	**2.92 Å**	**3.92 Å**	**4.92 Å**
1	28.262	27.124	26.555	20.106	19.347	18.854
2	25.417	24.279	23.900	18.266	17.469	17.185
3	34.142	32.814	32.245	42.298	40.591	39.833
4	139.604	124.429	117.411	202.956	182.281	172.228
5	70.561	75.872	75.872	80.234	80.424	78.717

Orientation: Cyano

	Linear			Circular		
Ex. no	**3.27 Å**	**4.27 Å**	**5.27 Å**	**3.27 Å**	**4.27 Å**	**5.27 Å**
1	41.540	33.383	29.780	28.641	23.520	21.054
2	15.326	19.537	21.434	10.698	13.847	15.326
3	33.763	31.866	31.676	44.954	41.160	40.212
4	195.369	136.379	122.533	282.621	204.853	182.471
5	1354.307	220.027	132.016	1014.782	193.472	121.963

Orientation: Amino

	Linear			Circular		
Ex. no	**2.92 Å**	**3.92 Å**	**4.92 Å**	**2.92 Å**	**3.92 Å**	**4.92 Å**
1	51.213	34.142	31.866	23.141	23.900	22.572
2	23.900	22.572	21.813	18.001	16.218	15.573
3	286.415	41.350	36.039	265.550	49.506	44.764
4	66.388	149.657	129.551	69.043	218.131	189.679
5	176.591	65.629	125.947	254.170	63.163	112.669

Table 18: The two-photon cross-section, in a.u., of *s-trans*-VHF with copper nanoparticle for all the orientations and molecule-nanoparticle distances.

Orientation: 7-membered

	Linear			Circular		
Ex. no	**2.60 Å**	**3.60 Å**	**4.60 Å**	**2.60 Å**	**3.60 Å**	**4.60 Å**
1	41.54	33.573	29.969	29.211	23.710	21.244
2	17.375	20.675	22.003	12.576	14.757	15.705
3	56.714	41.16	36.039	65.819	49.696	44.385
4	158.002	133.724	122.343	231.408	197.266	180.005
5	512.133	199.163	123.86	404.016	175.074	116.083

Orientation: Phenyl

	Linear			Circular		
Ex. no	**2.60 Å**	**3.60 Å**	**4.60 Å**	**2.60 Å**	**3.60 Å**	**4.60 Å**
1	34.522	30.918	28.641	24.658	22.003	20.485
2	23.33	23.52	23.52	16.749	16.787	16.787
3	37.746	35.28	33.763	47.989	44.195	42.109
4	153.64	131.068	120.825	227.615	193.472	178.488
5	153.071	121.394	99.392	148.708	116.842	97.305

Orientation: Cyano

	Linear			Circular		
Ex. no	**2.92 Å**	**3.92 Å**	**4.92 Å**	**2.92 Å**	**3.92 Å**	**4.92 Å**
1	53.489	39.074	33.194	36.608	23.520	27.503
2	12.898	21.054	18.74	8.877	15.004	13.296
3	53.300	35.849	39.833	64.680	45.144	50.644
4	394.532	129.93	153.071	493.165	193.472	229.511
5	1.954×10^{5}	227.615	734.057	1.305×105	188.730	542.481

Orientation: Amino

	Linear			Circular		
Ex. no	**2.80 Å**	**3.60 Å**	**4.60 Å**	**2.80 Å**	**3.60 Å**	**4.60 Å**
1	515.926	60.508	45.144	311.073	41.729	31.487
2	39.074	13.562	16.749	25.417	9.465	11.817
3	1.083×10^{6}	64.491	44.195	7.170×10^{5}	78.717	56.145
4	4.382×10^{6}	358.493	177.539	2.921×10^{6}	485.578	265.55
5	1.201×10^{9}	5.596×10^{4}	1369.48^{1}	8.004×10^{8}	3.756×10^{4}	984.43^{3}

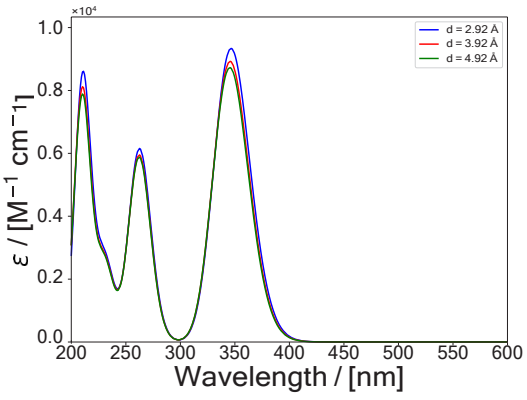

Figure 3: The simulated UV-Vis spectrum for the 7-membered orientation of DHA on the silver nanoparticle.

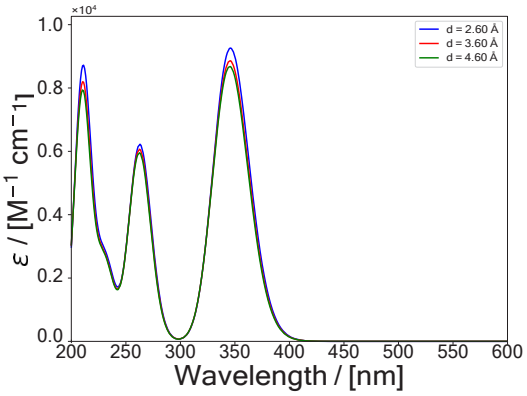

Figure 4: The simulated UV-Vis spectrum for the 7-membered orientation of DHA on the copper nanoparticle

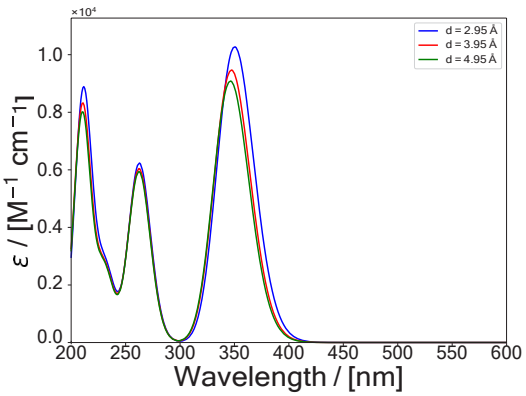

Figure 8: The simulated UV-Vis spectrum for the cyano orientation of DHA on the copper nanoparticle.

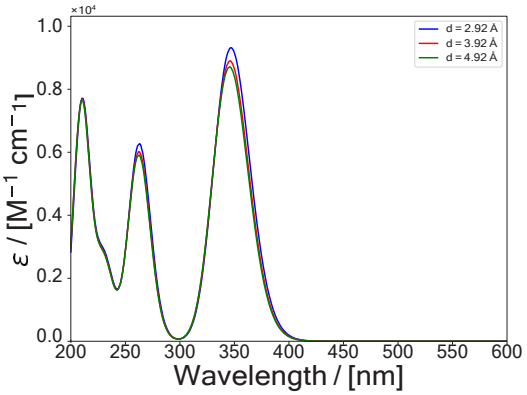

Figure 5: The simulated UV-Vis spectrum for the phenyl orientation of DHA on the silver nanoparticle.

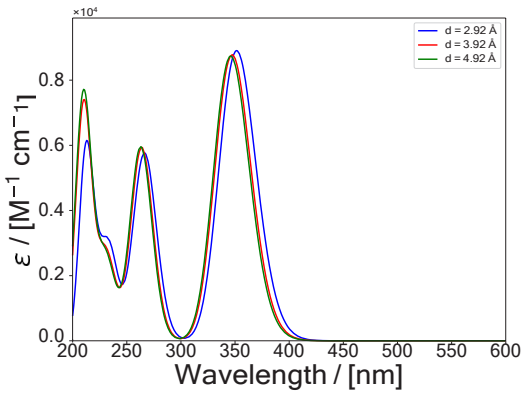

Figure 9: The simulated UV-Vis spectrum for the amino orientation of DHA on the silver nanoparticle.

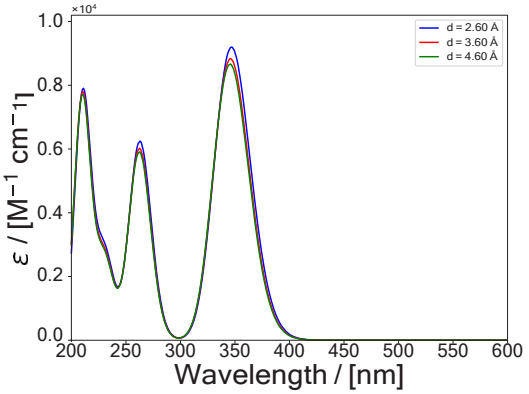

Figure 6: The simulated UV-Vis spectrum for the phenyl orientation of DHA on the copper nanoparticle.

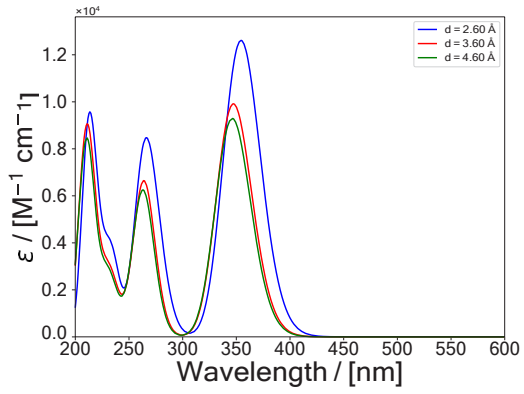

Figure 10: The simulated UV-Vis spectrum for the amino orientation DHA on the copper nanoparticle.

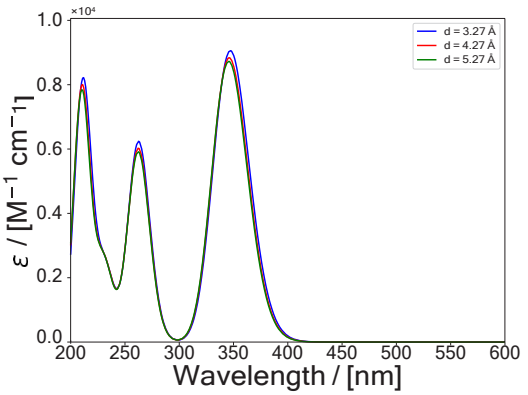

Figure 7: The simulated UV-Vis spectrum for the cyano orientation of DHA on the silver nanoparticle

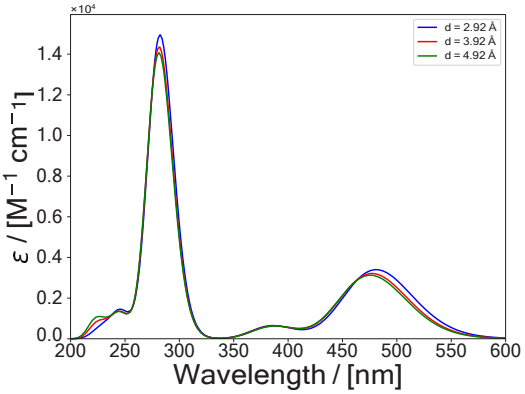

Figure 11: The simulated UV-Vis spectrum for the 7-membered orientation of s-cis-VHF on the silver nanoparticle.

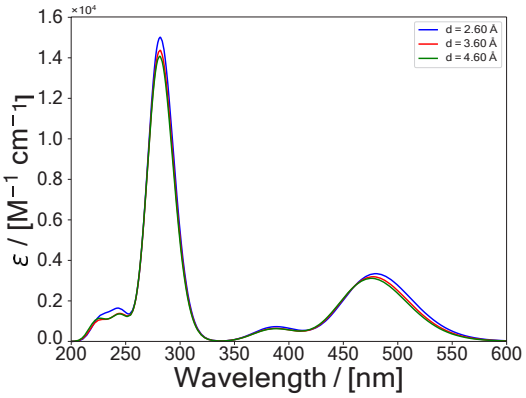

Figure 12: The simulated UV-Vis spectrum for the 7-membered orientation of s-cis-VHF on the copper nanoparticle.

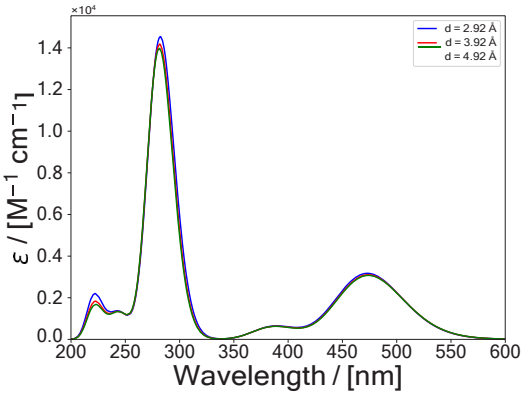

Figure 13: The simulated UV-Vis spectrum for the phenyl orientation of s-cis-VHF on the silver nanoparticle.

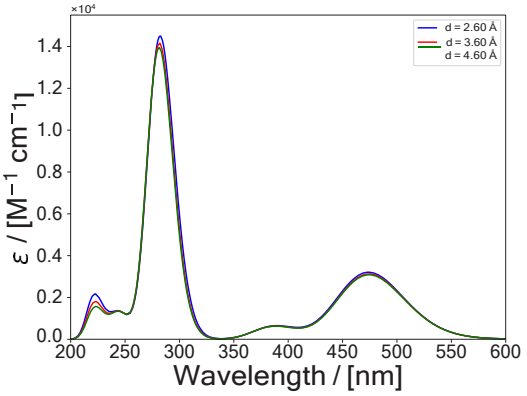

Figure 14: The simulated UV-Vis spectrum for the phenyl orientation of s-cis-VHF on the copper nanoparticle.

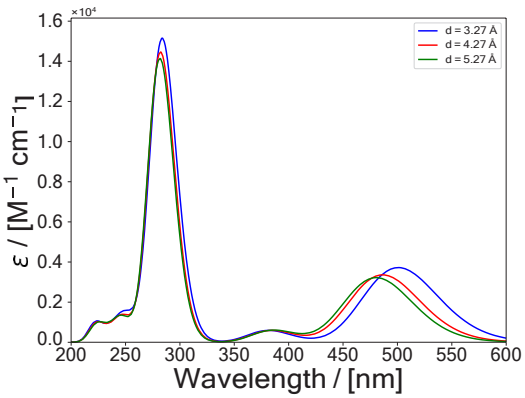

Figure 15: The simulated UV-Vis spectrum for the cyano orientation of s-cis-VHF on the silver nanoparticle.

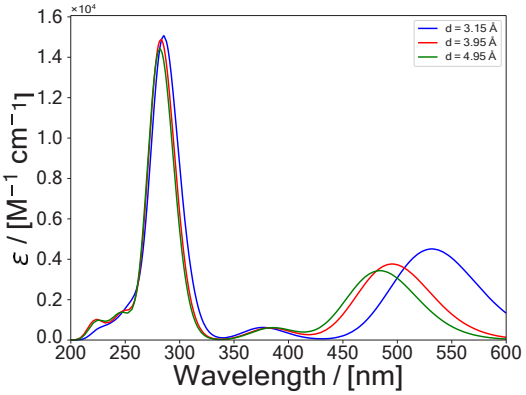

Figure 16: The simulated UV-Vis spectrum for the cyano orientation of s-cis-VHF on the copper nanoparticle.

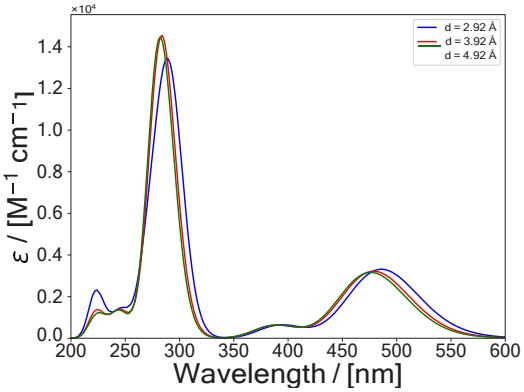

Figure 17: The simulated UV-Vis spectrum for the amino orientation of s-cis-VHF on the silver nanoparticle.

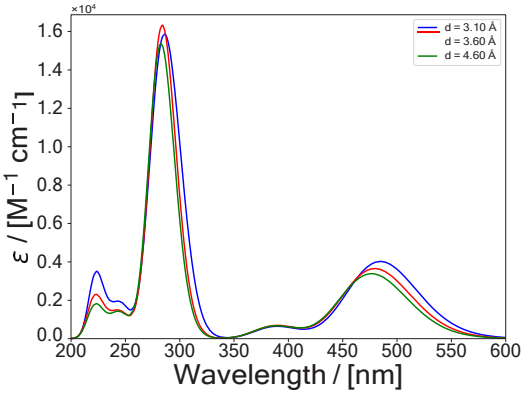

Figure 18: The simulated UV-Vis spectrum for the amino orientation of *s-cis*-VHF on the copper nanoparticle.

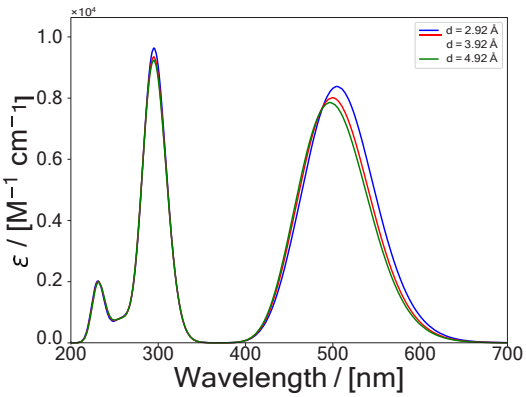

Figure 19: The simulated UV-Vis spectrum for the 7-membered orientation of s-trans-VHF on the silver nanoparticle.

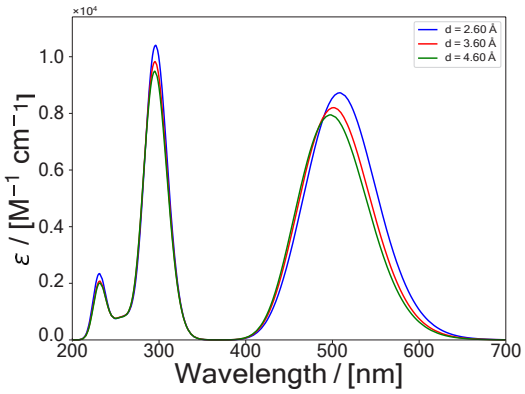

Figure 20: The simulated UV-Vis spectrum for the 7-membered orientation of s-trans-VHF on the copper nanoparticle.

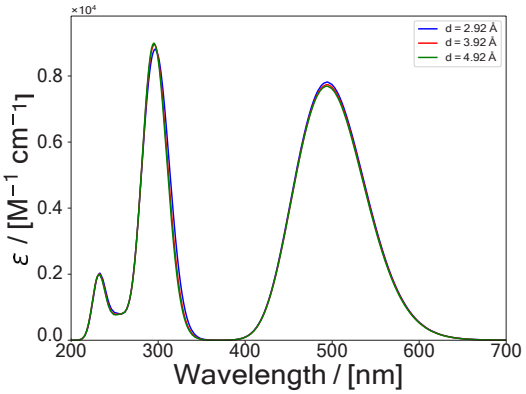

Figure 21: The simulated UV-Vis spectrum for the phenyl orientation of s-trans-VHF on the silver nanoparticle.

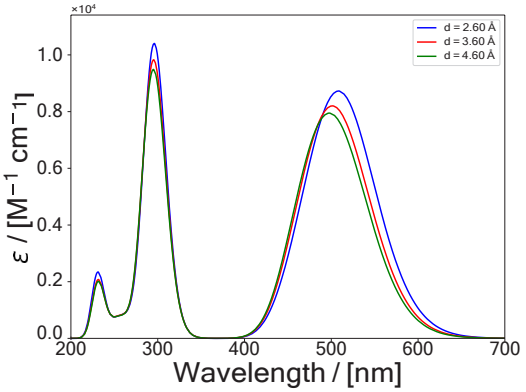

Figure 22: The simulated UV-Vis spectrum for the phenyl orientation of s-trans-VHF on the copper nanoparticle.

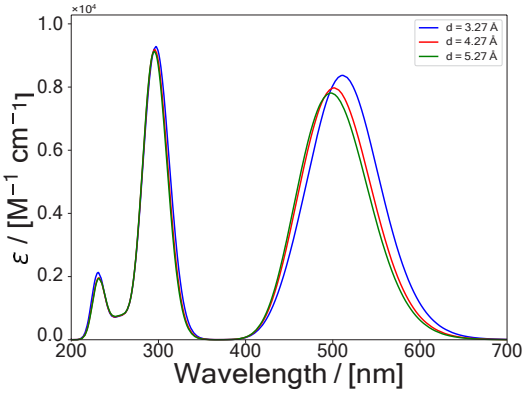

Figure 23: The simulated UV-Vis spectrum for the cyano orientation of *s-trans*-VHF on the silver nanoparticle.

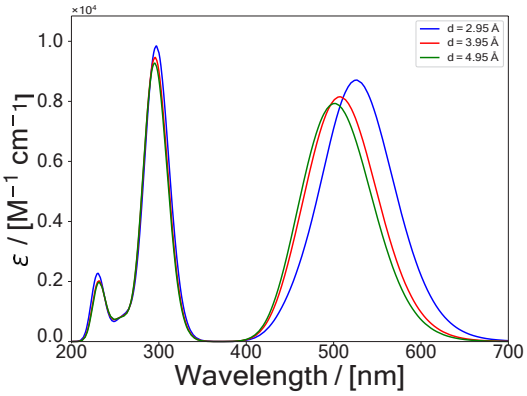

Figure 24: The simulated UV-Vis spectrum for the cyano orientation of *s-trans*-VHF on the copper nanoparticle.

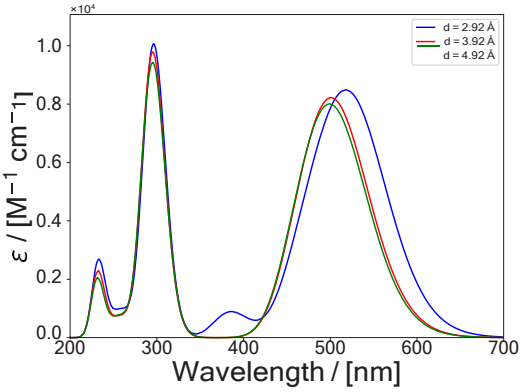

Figure 25: The simulated UV-Vis spectrum for the amino orientation of *s-trans*-VHF on the silver nanoparticle.

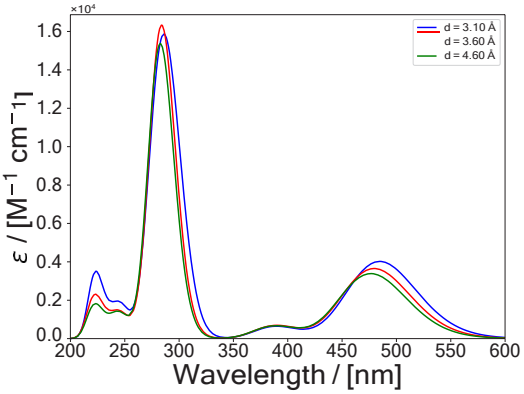

Figure 26: The simulated UV-Vis spectrum of the amino orientation of *s-trans*-VHF on the copper nanoparticle.

Conclusions

We have found that the inclusion of a nanoparticle to the DHA/VHF system has an impact on the molecular properties, in this case, the optical properties. It was found in general, that the copper nanoparticle has a greater impact on the optical properties as compared to the silver nanoparticle. However, both the silver and the copper nanoparticle have a larger effect when comparing with the gold nanoparticle from our previous work [35].

It is clear that the molecular choice, relative orientation, and molecule-nanoparticle distance all have a large impact on the effect from the nanoparticle. In particular it was found that when the two non-polar groups are facing the nanoparticle, the 7-membered and phenyl orientation, the nanoparticles have a

smaller effect on the one- and two photon absorptions. Furthermore, we observe the largest effects when the two polar groups are facing towards the nanoparticle, the cyano and amino orientation. The two polar orientations seem quite similar, with the amino orientation being influenced the most for the DHA and s-trans-VHF molecules, while the cyano orientation was influenced the most for the s-cis-VHF molecule. For the non-polar groups it was found that the 7-membered orientation has a slightly greater impact on the effect of the nanoparticle than the phenyl orientation. The different effects of the nanoparticle on the non-polar and polar groups facing towards the nanoparticle could be explained by the different dipoles of the groups. It could also be due to different overall molecular dipole orientation with respect to the nanoparticle, causing larger dipole interactions.

The nanoparticle has the greatest effect on the optical properties when the molecule- nanoparticle distance is small, which is what we expected. In general, we saw an increase in both UV-Vis absorption and two-photon cross-section when the distance was decreased. There were, however, some exceptions, where we observed a decrease in absorption in one region of the UV-Vis spectrum and an increase in another. In general we also saw a redshift when decreasing the molecule-nanoparticle distance, which was usually accompanied with an increase in absorption as well. We also observed cases where we have a redshift but no real increase in absorption and cases where we have no redshift but an increase in absorption.

It was also found that in general the s-trans-VHF molecule was the most affected by both nanoparticles and the DHA molecule was the least affected. This could also be due to a difference in dipole between the molecules.

Previous work has shown that polarizabilities and hyperpolarizabilities of the DHA/VHF system are also affected by the interactions with silver and copper nanoparticles [52]. It was shown that the linear and nonlinear polarizabilities depend strongly on the orientation of the physisorbed molecules and the distance between the molecule and the nanoparticle. The molecular properties increased significantly when the molecules have the polar groups pointing towards the nanoparticle and this can clearly be explained by considering the results in this manuscript. We observe that the excitation energies are decreased when the physisorbed molecules have the polar groups pointing towards the nanoparticles and the linear and nonlinear polarizabilities are proportional to the inverse of the excitation energies. We also observed that the linear and nonlinear polarizabilities are larger for the two conformations of VHF compared to DHA and again this observation is based on the much smaller excitation energies for the two VHF conformers. The effects of the copper nanoparticle on the molecular linear and nonlinear polarizabilities for the physisorbed molecules are for all orientations and distances larger than the effects due to the silver nanoparticle. Again this change is related to how the first excitation energies are changing as the physisorbed molecules interact with the nanoparticle and the excitation energies are lower when the three molecules interact with the copper nanoparticle.

These results are interesting and show that it might be possible to use nanoparticles to tune this system to obtain the desired optical properties for different application, such as solar cells and hopefully other molecular properties as well.

In the future, the description of the nanoparticles could, in particular, be improved. The nanoparticles are currently very small and as previously mentioned, the optical properties of the nanoparticle are also not currently included, excluding both plasmonic effects and absorption of the nanoparticle, which could have an effect on the results. The nanoparticle might absorb much of the light or different amounts depending on the molecule physisorbed onto it as well. In addition, only one molecule close to a nanoparticle is probably not an accurate description, so adding more molecules or a solvent might change the results as well.

Acknowledgement

This work was supported by the Center for Exploitation of Solar Energy, Department of Chemistry, University of Copenhagen, Denmark. K.V.M. acknowledges the Danish Council for Independent Research, DFF-0136-00081B, and the European Union's Horizon 2020 Framework Programme under grant agreement number 951801 for financial support. F. Ø. K. and A. E. H. B. would like to the thank the Danish Chemical Society for travel support to Pennsylvania State University.

Conflicts of interest: There are no conflicts to declare.

References

1. Daub J, Knochel T, Mannschreck A. Photosensitive Dihydroazulenes with Chro- mogenic Properties. Angew. Chem. Int. Ed. 1984; 23: 960-961.

2. Irie M. Diarylethenes for Memories and Switches. Chem. Rev. 2000; 100: 1685-1716.

3. Tian H, Yang S. Recent progresses on diarylethene based photochromic switches. Chem. Soc. Rev. 2004; 33: 85-97.

4. Russew MM, Hecht S. Photoswitches: From Molecules to Materials. Adv. Mater. 2010; 22: 3348-3360.

5. Plaquet A, Champagne B, Castet F, Ducasse L, Bogdan E, Rodriguez V, Pozzo JL. Theoretical investigation of the dynamic first hyperpolarizability of DHA- VHF molecular switches. New J. Chem. 2009; 33: 1349-1356.

6. Irie M, Fukaminato T, Matsuda K, Kobatake S. Photochromism of Diarylethene Molecules and Crystals: Memories, Switches, and Actuators. Chem. Rev. 2014; 114: 12174-12277. PMID: 25514509.

7. Broman SL, Nielsen MB. Dihydroazulene: from controlling photochromism to molecular electronics devices. Phys. Chem Chem Phys. 2014; 16: 21172-21182.

8. Kucharski TJ, Tian Y, Akbulatov S, Boulatov R. Chemical solutions for the closed-cycle storage of solar energy. Energy Environ. Sci. 2011; 4: 4449-4472.

9. Moth-Poulsen K, Coso D, Borjesson K, Vinokurov N, Meier SK, Majumdar A, Vollhardt KPC, Segalman, R. A. Molecular solar thermal (MOST) energy storage and release system. Energy Environ. Sci. 2012; 5: 8534-8537.

10. Broman SL, Petersen MA, Tortzen CG, Kadziola A, Kilsa K, Nielsen MB. Arylethynyl Derivatives of the Dihydroazulene/Vinylheptafulvene Photo/Thermoswitch: Tuning the Switching Event. J. Am. Chem. Soc. 2010; 132: 9165-9174.

11. Gorner H, Fischer C, Gierisch S, Daub J. Dihydroazulene/vinylheptafulvene pho- tochromism: effects of substituents, solvent, and temperature in the photorearrange- ment of dihydroazulenes to vinylheptafulvenes. J. Phys. Chem. 1993; 97: 4110-4117.

12. Gorner H, Fischer C, Daub J. Photoreaction of dihydroazulenes

into vinylheptaful- venes: photochromism of nitrophenyl-substituted derivatives. J. Photochem. Photobiol. A Chem. 1995; 85: 217 - 224.

13. Petersen MA˚, Broman SL, Kils˚a K, Kadziola A, Nielsen MB. Gaining Con- trol: Direct Suzuki Arylation of Dihydroazulenes and Tuning of Photo- and Ther- mochromism. Eur J Org Chem. 2011; 2011, 1033-1039.

14. Gierisch S, Bauer W, Gierisch T, Bauer J, Burgemeister S, Daub W. Substituent Dependency Of The Dihydroazulene-Reversible- Vinylheptafulvene Photochromism - Steric And Electronic Ef- Fects Of 9-Anthryl Compounds - New Access To Condensed Hy- Dropentalenes. Chem. Ber. 1989; 122: 2341-2349.

15. Schalk O, Broman SL, Petersen M˚A, Khakhulin DV, Brogaard RY, Nielsen MB, et al. On the Condensed Phase Ring-Closure of Vinylheptafulvalene and Ring-Opening of Gaseous Dihydroazulene. J. Phys. Chem. A 2013; 117: 3340-3347, PMID: 23556480.

16. Petersen M, Rasmussen B, Andersen NN, Sauer SPA, Nielsen MB, Beeren SR, et al. Molecular Switching in Confined Spaces: Effects of En- capsulating the DHA/VHF Photo-Switch in Cucurbiturils. Chem. Eur. J. 2017; 23: 17010-17016.

17. Vlasceanu A, Frandsen BN, Skov AB, Hansen AS, Rasmussen MG, Kjaer- gaard HG, et al. Photoswitchable Dihydroazulene Macrocycles for Solar Energy Storage: The Effects of Ring Strain. J. Org. Chem. 2017; 82: 10398-10407, PMID: 28853882.

18. Wang Z, Udmark J, Brjesson K, Rodrigues R, Roffey A, Abrahamsson M, et al. Evaluating Dihydroazulene/Vinylheptafulvene Pho- toswitches for Solar Energy Storage Applications. ChemSusChem 2017; 10: 3049-3055.

19. Skov AB, Petersen JF, Elm J, Frandsen BN, Santella M, Kilde MD, et al. Towards Storage of Solar Energy in Photochromic Molecules: Benzannulation of the Dihydroazulene/Vinylheptafulvene Couple. ChemPhotoChem 2017; 1: 206-212.

20. Gertsen AS, Olsen ST, Broman SL, Nielsen MB, Mikkelsen KV. A DFT Study of Multimode Switching in a Combined DHA/VHF-DTE/DHB System for Use in Solar Heat Batteries. J Phys Chem. C 2017; 121: 195-201.

21. Nisa RU, Shahzad N, Ayub K. Density functional theory study of linear and non- linear optical properties of dihydroazulene-vinylheptafulvene photoswitches. Comput. Theor Chem. 2016; 1095: 1 - 8.

22. Shahzad N, Nisa RU, Ayub K. Substituents effect on thermal electrocyclic re- action of dihydroazulenevinylheptafulvene photoswitch: A DFT study to improve the photoswitch. Struct. Chem. 2013; 24: 2115-2126.

23. Skov AB, Broman SL, Gertsen AS, Elm J, Jevric, M, Cacciarini M, et al. Aromaticity-Controlled Energy Storage Capacity of the Dihydroazulene-Vinylheptafulvene Photochromic System. Chem. Eur J. 2016; 22: 14567-14575.

24. Cacciarini M, Skov AB, Jevric M, Hansen AS, Elm J, Kjaergaard HG, et al. Towards Solar Energy Storage in the Photochromic DihydroazuleneVinylheptafulvene System. Chem Eur J. 2015; 21: 7454-7461.

25. Petersen AU, Broman SL, Olsen ST, Hansen AS, Du L, Kadziola A, et al. Controlling Two- Step Multimode Switching of Dihydroazulene Photoswitches. Chem. Eur. J 2015; 21: 3968-3977.

26. Petroleum BBP. Statistical Review of world energy 2015. Statistical review of world energy 2015, 2016: 65.

27. Hansen MH, Elm J, Olsen ST, Gejl AN, Storm FE, Frandsen BN, et al. Theoretical Investigation of Substituent Effects on the Dihydroazulene/Vinylheptafulvene Photoswitch: Increasing the Energy Storage Capacity. J Phys Chem. A 2016; 120: 9782-9793.

28. Ree N, Hansen MH, Gertsen AS, Mikkelsen K.V. Density Functional Theory Study of the Solvent Effects on Systematically Substituted Dihydroazu- lene/Vinylheptafulvene Systems: Improving the Capability of Molecular Energy Stor- age. J Phys Chem. A 2017; 121: 8856-8865.

29. Perrier A, Tesson S, Jacquemin, D, Maurel F. On the photochromic properties of dithienylethenes grafted on gold clusters. Comput. Theor. Chem. 2012; 990: 167-176.

30. Klajn R, Stoddart JF, Grzybowski BA. Nanoparticles functionalised with re- versible molecular and supramolecular switches. Chem. Soc. Rev 2010; 39: 2203-2237.

31. Mahmoodi NO, Ahmadi NK, Ghavidast A. Light-induced switching of 1, 3- diazabicyclo-[3.1. 0] hex-3-enes on gold nanoparticles. J Mol Struct. 2018; 1160: 463- 470.

32. Ghavidast A, Mahmoodi NO. A comparative study of the photochromic compounds incorporated on the surface of nanoparticles. J Mol Liq. 2016; 216: 552-564.

33. Perrier A, Maurel F, Aubard J. Theoretical study of the electronic and optical properties of photochromic dithienylethene derivatives connected to small gold clusters. J Phys Chem. A 2007; 111: 9688-9698.

34. Boye IMI, Hansen MH, Mikkelsen KV. The influence of nanoparticles on the polarizabilities and hyperpolarizabilities of photochromic molecules. Phys. Chem. Chem. Phys. 2018; 20: 23320-23327.

35. Hillers-Bendtsen AE, Hansen MH, Mikkelsen KV. The influence of nanoparticles on the excitation energies of the photochromic dihydroazulene/vinylheptafulvene (DHA/VHF) system. Phys. Chem. Chem. Phys. 2019.

36. Bakowies D, Thiel W. Hybrid models for combined quantum mechanical and molec- ular mechanical approaches. J. Phys. Chem. 1996; 100: 10580-10594.

37. Olsen JM, Aidas K, Kongsted J. Excited states in solution through polarizable embedding. J. Chem. Theory Comput. 2010; 6: 3721-3734.

38. Poulsen TD, Kongsted J, Osted A, Ogilby PR, Mikkelsez KV. The combined multiconfigurational self-consistent-field/molecular mechanics wave function approach. J. Chem. Phys. 2001; 115: 2393-2400.

39. Kongsted J, Osted A, Mikkelsen KV, Christiansen O. The QM/MM approach for wavefunctions, energies and response functions within self-consistent field and coupled cluster theories. Mol Phys. 2002; 100: 1813-1828.

40. Poulsen TD, Ogilby PR, Mikkelsen KV. A quantum mechanical method for cal- culating nonlinear optical properties of condensed phase molecules coupled to a molecular mechanics field: A quadratic multiconfigurational self-consistent-field/molecular mechanics response method. J Chem Phys. 2001; 115, 7843-7851.

41. Aidas K, Angeli C, Bak KL, Bakken V, Bast R, Boman L, et al. The Dalton quantum chemistry program system. WIREs Comput. Mol. Sci. 2014; 4: 269-284.

42. Frisch MJ, Trucks GW, Schlegel HB, Scuseria GE, Robb MA, Cheese-man JR, et al. Gaussian09 Revision D.01. Gaussian Inc. Wallingford CT 2009.

43. Yanai T, Tew DP, Handy NC. A new hybrid exchange-correlation functional using the Coulomb-attenuating method (CAM-B3LYP). Chem. Phys. Lett. 2004; 393: 51-57.

44. Wilson AK, van Mourik T, Dunning Jr TH. Gaussian basis sets for use in cor- related molecular calculations. VI. Sextuple zeta correlation consistent basis sets for boron through neon. J Mol Struct. Theochem. 1996; 388: 339-349.

45. Olsen ST, Bols A, Hansen T, Mikkelsen KV. Molecular Properties of Sandwiched Molecules Between Electrodes and Nanoparticles. 2017; 75: 53-102.

46. Ceperley DM, Alder BJ. Ground State of the Electron Gas by a Stochastic Method. Phys Rev Lett. 1980; 45, 566-569.

47. Bili´c A, Reimers JR, Hush NS. The structure, energetics, and nature of the chem- ical bonding of phenylthiol adsorbed on the Au(111) surface: Implications for density- functional calculations of molecular-electronic conduction. J Chem Phys. 2005; 122: 094708.

48. Pereiro M, Baldomir D. Structure and static response of small silver clusters to an external electric field. arXiv preprint physics. 2007; 0702238.

49. Sarkisov G, Hamilton A, Sotnikov V. Dynamic dipole polarizability of gold and copper atoms for 532-and 1064-nm wavelengths. Phys. Rev. 2019; 99: 012503.

50. Jaque P, Toro-Labb´e A. Characterization of copper clusters through the use of density functional theory reactivity descriptors. J Chem Phys. 2002; 117: 3208-3218.

51. Knickelbein MB. Electric dipole polarizabilities of copper clusters. J Chem Phys. 2004; 120: 10450-10454.

52. Hillers-Bendtsen AE, Kjeldal FØ, Mikkelsen KV. Electric properties of pho- tochromic molecules physisorbed on silver and copper nanoparticles. Phys Chem. A 2023, 126, 3145-3156. -> J Phys Chem. A 2023, 126, 3145-3156.